PHYSICAL REVIEW B VOLUME 55, NUMBER 24 15 JUNE 1997-II

Anomalous plastic deformation at surfaces: Nanoindentation of gold single crystals

S. G. Corcoran* and R. J. Colton
Naval Research Laboratory, Code 6177, Washington, D.C. 20375-5342

E. T. Lilleodden and W. W. Gerberich
University of Minnesota, Department of Chemical Engineering and Materials Science, Minneapolis, Minnesota 55455-0132

(Received 14 April 1997)

Nanoindentation data on single-crystal Au(111), Au(110), and Au(100) are presented and show an interesting yielding phenomenon—this yielding behavior is composed of a series of discrete yielding events separated by elastic deformation. The onset of this behavior is in agreement with calculations for the theoretical shear strength of gold. Good quantitative agreement is found between the experimental results and a model developed for the nucleation and multiplication of dislocations by a simple Frank-Read source under the indenter tip. [S0163-1829(97)51324-5]

A better understanding of the mechanics associated with the contact of small volumes is becoming increasingly important from both a scientific and technological viewpoint. The results of such research have widespread implications in such areas as device miniaturization, computer disk drive technology, and fracture mechanics as related to the understanding of crack tip blunting by dislocation emission. The recent advances in nanoindentation techniques has allowed for the detailed investigation of the contact of small volumes where the contact radius is less than 100 nm. Since a typical dislocation separation is of order 1 μm for well-annealed metals, the area under the nanoindenter should behave close to that of a perfect single crystal, i.e., dislocation free. In fact, Gane and Bowden[1] noted that a metal's resistance to indentation on a small scale was quite different than the conventional microhardness measurements. They observed that a critical load must be reached before a stylus could penetrate into the surface of a Au crystal. The critical load approached that of the theoretical shear strength of the crystal, although the authors report quite a variability in the load, most likely the result of organic impurities adsorbed on the Au surface.

Recently, discontinuities in displacement have been observed during nanoindentation in many systems but we will confine our discussion to those observed on metal surfaces.[2–9] These displacement excursions have been attributed typically to oxide breakthrough by dislocations or an effect of some unknown contamination layer on the metal surface. Gerberich *et al.*[7] demonstrated the existence of a second displacement excursion at very low loads for the system Fe–3 wt % Si which was interpreted as an indication of dislocation emission below the oxide film prior to oxide breakthrough. Motivated by this finding and the yield instabilities originally observed on Au by Gane and Bowden[1] via scanning electron microscopy we investigated the yield behavior of well-prepared single-crystal Au which was free of any surface oxides or contamination layers. We find that the three low index faces of Au exhibit a reproducible displacement excursion near the theoretical yield strength for gold in agreement with a dislocation nucleation event. In fact, an interesting yielding phenomenon was observed in which the plasticity was confined to a series of excursions separated by elastic deformation. As many as two excursions have been observed by previous authors;[7,10] however, we are unaware of previous clear evidence for a series of displacement excursions separated by elastic loading. We believe that such behavior is indicative of the contact of small volumes where the linear dimension of the plastic volume is less than the average dislocation spacing. A simple model based on the nucleation and activation of a Frank-Read source under the indenter tip is evaluated and compared to the experimental results.

A commercial Hysitron, Inc. Picoindenter® was used on conjunction with the Digital Instruments, Nanoscope™ III atomic force microscope AFM/scanning tunnel microscope (STM) to perform indentations on Au single crystals oriented in the [111], [110], and [100] directions. The specially designed force transducer of Hysitron, Inc. allows for the direct imaging of the surface before and after the indentation exactly centered over the point of contact. A Berkovich diamond indenter was used for all indentations. The blunt end of the indenter had a spherical radius of approximately 205 nm as determined by imaging the tip with an asperity on the Au surface.[8] The indenter tip is engaged on the surface in an AFM imaging mode with a load of typically 800 nN. The surface is imaged with the indenter tip and, a site other than the impact site is chosen for the indentation avoiding any deformation associated with the initial impact.[11]

The gold single crystals[12] (99.99%) were prepared immediately before each series of indentations by electrochemical polishing at 2.5 A in a 1:2:1 electrolyte of ethylene glycol: ethanol:HCl at 55 °C. The surfaces were then flame annealed until glowing red hot under a H_2 flame. The samples were then quenched and stored under triply distilled water and transferred into a dry N_2-purged glove bag where the indentation experiments were conducted. The N_2 flowed through a column of $CaSO_4$ and 5 nm molecular sieve to eliminate H_2O and organic impurities. The flame annealing technique was developed by Clavilier *et al.*[13] and is used extensively in the electrochemical scanning tunneling microscopy community to produce clean Au surfaces (better than submonolayer contamination) with atomically flat terraces of a few 100 nm

in width. As a control, we removed some Au samples from the distilled water for several hours prior to indentation testing. For these samples, we obtained very irreproducible results and increased values of hardness.[8] X-ray photoemission spectroscopy results for this ''dirty'' Au surface revealed the presence of a single monolayer of carbonaceous contamination. From these results, and the fact that we get complete reproducibility on clean surfaces we feel confident that our surface-preparation procedure produces surfaces with better than submonolayer contamination.

Figure 1 shows the typical load-displacement curves obtained for the Au (111), (100), and (110) crystals, respectively. The first displacement excursion corresponds to the initiation of plastic deformation (yield point). Before this excursion, only elastic deformation is observed as confirmed by direct imaging the surface before and after indentation with the Hysitron indenter and also by unloading before the onset of the first excursion as shown in the Au (100) inset of Fig. 1.

The value of the yield point was sensitive to the degree of surface roughness. For the (111) crystal where atomic terraces 15 nm wide were separated by single atomic steps 0.24 nm in height, a typical yield point of 8 μN ($\sim$3 GPa) was obtained. The area of contact between the indenter and Au surface is obtained by assuming Hertzian contact up to the first yield excursion for a spherical tip with a radius of 205 nm. This radius was determined by direct imaging of the tip in the AFM mode of the Hysitron instrument. For the (100) crystal, a typical value of 44 μN (8.5 GPa) was obtained on atomically flat terraces 200–300 nm in width but very quickly approached values closer to that of the (111) crystal as the surface roughness increased. Similar behavior was observed for the (110) crystal. Owing to the large dependence of the yield point on the surface roughness, no orientational dependence for the yield point was resolved. Regardless, even the smallest value of the yield point approached that of the theoretical shear strength of Au and is significantly greater than the critical resolved shear stress τ_R of single crystal Au equal to 0.9 MPa.[14] If we take the theoretical shear strength τ_c of Au to be equal to $G_s/2\pi$ where G_s is the shear modulus (30 GPa), we get a τ_c of approximately 5 GPa. Assuming that τ_R is equal to the maximum shear stress under the indenter (0.45 of the mean pressure) we get τ_R in the range of 1.5–4 GPa which is quite close to the theoretical shear strength of 5 GPa.

The load-displacement curves of Fig. 1 also show the discrete-yielding-event phenomenon. This yielding behavior is unique because the plasticity appears to be confined to particular values of the displacement, i.e., the Au surface predominantly deforms elastically between each yield excursion. We note that the number of such displacement excursions, as well as their size, varies between indentations, but the sum total of all displacements is conserved, i.e., the average shape of the indentation curve is highly reproducible. The significance of the elastic loading and unloading after a yield event is that an apparent force equilibrium is set up between the dislocations and the indenter which makes the indenter behave as if it were in an elastic medium. We should point out that all data shown are the raw data, i.e., no drift corrections were necessary. Drift was insignificant with the Hysitron instrument once thermal equilibrium was reached (typically 1 h) as evident in the reversibility of the inset of Au (100) in Fig. 1. For some of the data in Fig. 1 the initial unloading slope is slightly negative. This is due to the significant creep that occurs for well-annealed Au surfaces.

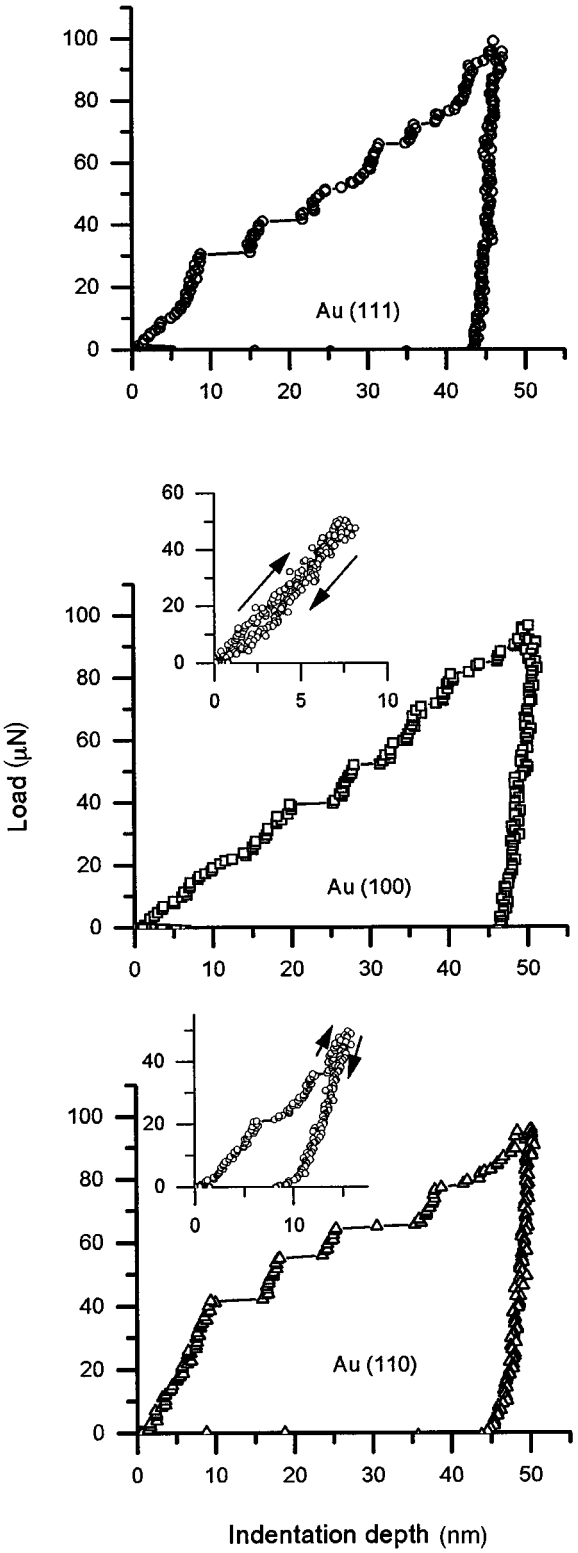

FIG. 1. Typical load-displacement curves for Au single crystals (111), (100), and (110). The inset of Au (100) is a load-displacement curve for Au (100) showing elastic loading and unloading just prior to the first displacement excursion. The inset of Au (110) is a load-displacement curve for Au (110) showing elastic loading and unloading just prior to the next displacement excursion.

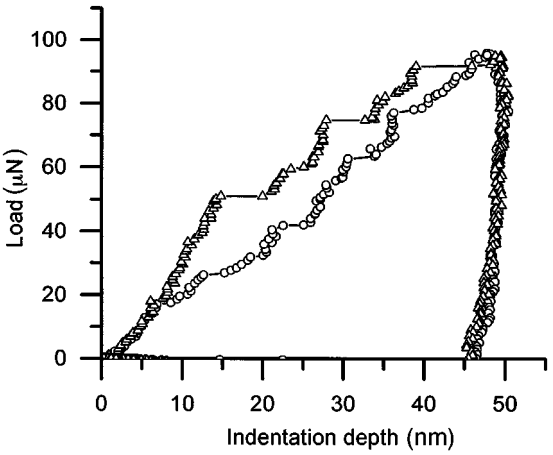

FIG. 2. Load-displacement curve for Au (100) when the indenter is centered over an atomically flat terrace (△) or over step bunches (○).

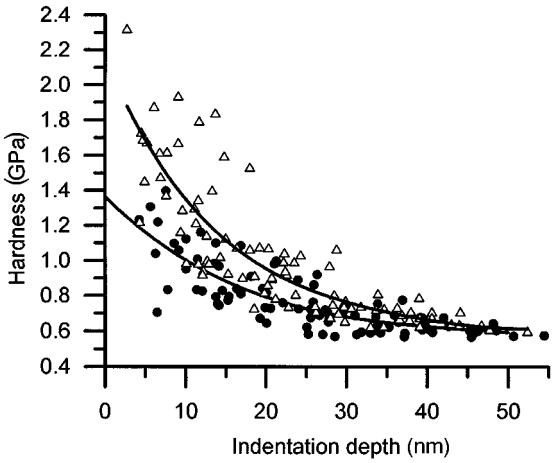

FIG. 3. Hardness values obtained from indentation curves taken for the Au (100) surface. The hardness values were obtained by dividing the load at excursion i by the geometric area of the indenter at a depth equivalent to the indentation depth before (△) and after (●) excursion i.

The inset of Au (110) in Fig. 1 shows an example of a loading cycle in which the unloading portion of the curve occurs just before the next displacement excursion. The initial unloading approximately traces the upper portion of the loading curve indicating elastic behavior.

The presence of surface atomic steps had a marked influence on the load-displacement response. Figure 2 shows the effect of performing an indent on a step bunch approximately 2 nm in height as compared to indenting on an atomically flat area[15] with the identical indenter tip. We believe the atomic steps act as nucleation sites for dislocations owing to the decrease in surface energy associated with annihilating step edges. The opposite case would be true for an atomically flat surface in which atomic steps must be created. For the analogous problem of crack tip blunting, this edge energy can dominate the dislocation emission criterion.[16]

The presence of displacement excursions for nanometer scale contacts suggests a further difficulty in quantifying the behavior of materials with a simple number such as the hardness. With discrete yielding events, substantially different values for hardness would be obtained depending upon whether an indenter was unloaded before or after a displacement excursion as shown in Fig. 3. For comparison, the typical hardness value for polycrystalline Au obtained by conventional microhardness testing is 300 MPa.[14] Literature values for the hardness of Au obtained by nanoindentation are 650 MPa (Ref. 17) and 2 GPa,[18] which spans the range of hardness values in Fig. 3.

We now analyze the yielding phenomenon following an analysis performed previously[7] for a single displacement excursion. In the model, it is assumed that a single displacement excursion is initiated by a single dislocation nucleation event. This first dislocation then acts as a Frank-Read (F-R) source eventually creating a dislocation pileup under the indenter. This source will operate until the back forces from the inverse pileup are sufficient to sum the forces to zero. This marks the end of the displacement excursion. The sample is then further loaded until another source is created on a parallel slip band; this marks the beginning of the next excursion. If we assume that the F-R source has pinning points separated by a length equal to the contact diameter, $2a$ (Ref. 19) and ignore lattice friction and image forces we can write the force balance (in units of force/length) of one such pileup as

$$\tau_R(r_S)b - \frac{G_S b^2}{2a} - \frac{G_S N b^2}{2\pi(r_S - a)} = 0, \tag{1}$$

where $\tau_R(r_S)$ is the critical resolved shear stress, b is the Burgers vector, G_S is the shear modulus, a is the contact radius, N is the number of dislocations in the pileup, and r_S is the position of the superdislocation. The first term represents the shear stress operating on the F-R source by the externally applied load; the second term is the critical force necessary to operate a source of length $2a$; and the third term is the sum of all of the forces of the dislocations in the pileup acting on the first dislocation written in terms of a single superdislocation of strength Nb located at distance r_S. If we take $\tau_R(r_S)$ to be the maximum shear stress under the indenter at depth r_S and load P_{yp}, we can rewrite Eq. (1) as

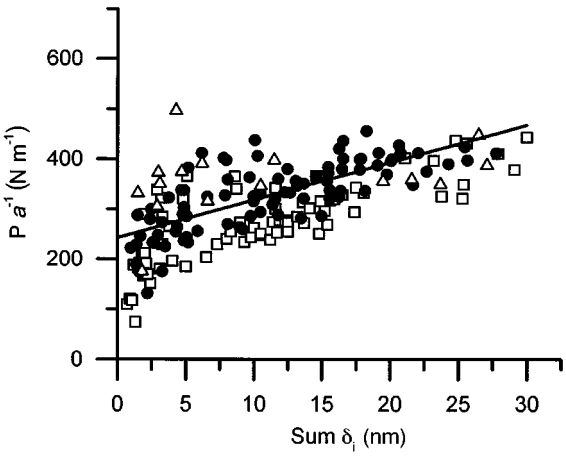

FIG. 4. Normalized load $P_i a^{-1}$ at excursion i, vs the sum of all displacements from excursions 1 through i [□, Au (111); ●, Au (100); and △, Au (110)].

$$P_{yp}=\frac{3\pi a}{2C(\alpha)}\left\{\frac{G_S b}{2}\left[1+\frac{N}{\pi(\alpha-1)}\right]\right\} \tag{2}$$

where $C(\alpha)$ is a geometric term equal to 0.119 for $\alpha=4$, where α is the position of the super dislocation Nb in units of the contact radius a. If we assume that all of the plasticity is confined to the displacement excursions of size δ and we take $N\approx\delta/b$, then Eq. (2) should apply to displacement excursion i if N is taken as $\Sigma\delta_i/b$ for all excursions up to load P_i. For $G_s=30$ GPa, $\alpha=4$, $C(\alpha)=0.119$, we get

$$\frac{P_{yp}}{a}=174\ \mathrm{N\ m^{-1}}+64\ \mathrm{GPa}\Sigma\,\delta_i\,. \tag{3}$$

Figure 4 is a plot of the load at excursion i, normalized by the contact radius a versus the sum of all excursions 1 to i for Au (111), (100), and (110). Linear regression using all of the data yields the equation

$$\frac{P_{yp}}{a}=242\ \mathrm{N\ m^{-1}}+7.5\ \mathrm{GPa}\Sigma\,\delta_i\,. \tag{4}$$

The constant in the above equation, which is directly related to the stress necessary to activate the Frank-Read source, is in fairly good agreement with the predicted value of Eq. (3). However, the experimentally determined slope is significantly less than the predicted value. This discrepancy is to be expected since this simplified model does not take into account the interaction of dislocations on parallel slip bands. For the ''particular'' yielding behavior we observed in Au, we can visualize each excursion as that of the activation of a parallel slip band. Shielding effects between the dislocations in these parallel slip bands would result in an overestimation of the applied load. That is, a parallel set of slip bands is not as effective at supporting the applied load as a single band and of course the actual distribution of dislocations under an indenter tip is much more complicated than this simple view after perhaps only a few excursions.

S.G.C. acknowledges the NRC for financial support. S.G.C. and R.J.C. acknowledge Hysitron, Inc. for their technical assistance and ONR for support. W.W.G. and E.T.L. acknowledge support by the Center for Interfacial Engineering under Grant No. NSF/CDR-8721551.

*Author to whom correspondence should be addressed. Present address: Hysitron, Inc., Nanomechanics Research Lab., 2010 E. Hennepin Avenue, Minneapolis, MN, 55413. Electronic address: corcoran@hysitron.com

[1] N. Gane and F. P. Bowden, J. Appl. Phys. **39**, 1432 (1968).

[2] P. Tangyunyong, R. C. Thomas, J. E. Houston, T. A. Michalske, R. M. Crooks, and A. J. Howard, Phys. Rev. Lett. **71**, 3319 (1993).

[3] W. C. Oliver and G. M. Pharr, J. Mater. Res. **7**, 1564 (1992).

[4] S. K. Venkataraman, D. L. Kohlstedt, and W. W. Gerberich, J. Mater. Res. **8**, 685 (1993).

[5] W. W. Gerberich, S. K. Venkataraman, H. Huang, S. E. Harvey, and D. L. Kohlstedt, Acta Metall. Mater. **43**, 1569 (1995).

[6] E. Lilleodden, W. Bonin, J. Nelson, and W. W. Gerberich, J. Mater. Res. Commun. **10**, 2162 (1995).

[7] W. W. Gerberich, J. C. Nelson, E. T. Lilleodden, P. Anderson, and J. T. Wyrobek, Acta Metall. Mater. **44**, 3585 (1996).

[8] S. G. Corcoran, R. J. Colton, E. T. Lilleodden, W. W. Gerberich (unpublished).

[9] J. B. Pethica and W. C. Oliver, in *Thin Films: Stresses and Mechanical Properties* edited by J. C. Bravman *et al.*, MRS Symposia Proceedings No. 130 (Materials Research Society, Pittsburgh, 1989), p. 13.

[10] T. F. Page, W. C. Oliver, and C. J. McHargue, J. Mater. Res. **7**, 450 (1992).

[11] A. B. Mann and J. B. Pethica, Appl. Phys. Lett. **69**, 907 (1996).

[12] Monocrystals, Inc. Cleveland, OH.

[13] J. Clavilier, R. Faure, G. Guinet, and R. Durand, J. Electroanal. Chem. **107**, 205 (1980).

[14] A. S. Argon, in *Mechanical Behavior of Materials*, edited by F. A. McClintock and A. S. Argon (Addison-Wesley, Reading, MA, 1966), p. 130.

[15] An atomically flat area may contain single atomic steps which would be beyond the resolution capable with the Berkovich tip used for imaging.

[16] S. J. Zhou, A. E. Carlsson, and R. Thomson, Phys. Rev. Lett. **72**, 852 (1994); K. Sieradzki and R. C. Cammarata, *ibid*. **73**, 1049 (1994).

[17] N. A. Burnham and R. J. Colton, J. Vac. Sci. Technol. A **7**, 2906 (1989).

[18] W. C. Oliver, R. Hutchings, and J. B. Pethica, in *Microindentation Techniques in Materials Science and Engineering*, edited by P. J. Blau and B. R. Lawn (American Society for Testing and Materials, Philadelphia, 1986), pp. 90–108.

[19] For large indenter radii, the dislocation loops created would have a radius less than the contact radius. However, for small indentations, $\delta\sim$10–40 nm and tip radii $\sim$200 nm, the contact radius is on the order of 100 nm which is not at all unrealistic for dislocation loop nucleation. For example, Page, Oliver, and McHargue (Ref. 10) found loops on the order of 200 nm in size for 50-nm-deep indents into sapphire.